Supplemental Information

Adipocyte CB1 receptor regulates energy homeostasis and alternatively activated macrophages

Inigo Ruiz de Azua[1,12,13], Giacomo Mancini[1,12], Raj Kamal Srivastava[1,12], Alejandro Aparisi Rey[1], Pierre Cardinal[2,3], Laura Tedesco[4], Cristina Maria Zingaretti[5], Antonia Sassmann[6], Carmelo Quarta[7], Claudia Schwitter[1], Andrea Conrad[1], Nina Wettschureck[6], V. Kiran Vemuri[8], Alexandros Makriyannis[8], Jens Hartwig[9], Maria Mendez-Lago[9], Laura Bindila[1], Krisztina Monory[1], Antonio Giordano[5], Saverio Cinti[5], Giovanni Marsicano[2,3], Stefan Offermanns[6], Enzo Nisoli[4], Uberto Pagotto[10], Daniela Cota[2,3], Beat Lutz[1,11,13]

[1]Institute of Physiological Chemistry, University Medical Center of the Johannes Gutenberg University of Mainz, Mainz 55128, Germany.
[2]INSERM U1215, Neurocentre Magendie, Bordeaux 33077, France.
[3]University of Bordeaux, Bordeaux 33077, France.
[4]Center for Study and Research on Obesity, Department of Medical Biotechnology and Translational Medicine University of Milan, Milan 20129, Italy.
[5]Department of Experimental and Clinical Medicine, Center of Obesity, University of Ancona (Politecnica delle Marche) Ancona 60020, Italy.
[6]Department of Pharmacology, Max Planck Institute for Heart and Lung Research, Bad Nauheim 61231, Germany.
[7]Helmholtz Diabetes Center (HDC) & German Center for Diabetes Research (DZD), Helmholtz Zentrum München, 85764 Neuherberg, Germany; Division of Metabolic Diseases, Technische Universität München, 80333 Munich, Germany.
[8]Center for Drug Discovery, Departments of Pharmaceutical Sciences & Chemical Biology, Northeastern University, Boston, MA 02115, USA.
[9]Institute of Molecular Biology (IMB), 55128 Mainz, Germany.
[10]Endocrinology Unit and Centro di Ricerca Biomedica Applicata, Department of Medical and Surgical Sciences, S.Orsola-Malpighi Hospital, Alma Mater University of Bologna, Bologna 40138, Italy.
[11]German Resilience Center, University Medical Center of the Johannes Gutenberg University of Mainz, Mainz 55131, Germany.

[12]Shared equal contributions
[13]Correspondence to Beat Lutz (Institute of Physiological Chemistry, Mainz 55128, Germany; Tel. +49 6131 39 25912; Email: blutz@uni-mainz.de) or Inigo Ruiz de Azua (Institute of Physiological Chemistry, Mainz 55128, Germany; Tel. +49 6131 39 25912; Email: inigo.azua@uni-mainz.de)

Supplemental Figure Legends

Supplemental Figure 1. *CB1* gene deletion in adipocytes. (A) Schematic representation of *CB1* floxed allele to generate adipocyte-specific *CB1*-deficient mice. Open box: *CB1* open reading frame encoding the CB1 protein; triangles: loxP sites; arrows: primers for polymerase chain reaction (PCR) genotyping (see Methods for primer sequences). **(B)** PCR analysis of the *CB1* gene locus by using the three primers G50, G51, and G53 on genomic DNA from epididymal fat (EF), subcutaneous fat (SF), brown adipose tissue (BAT), hypothalamus, soleus muscle and liver of $CB1^{fl/fl;AdipoqCreERT2tg/+}$ mice without (gel on the left) and following tamoxifen (+Tam) administration and recombination (gel on the right), respectively. Note that the *AdipoqCreERT2* transgene was always present in a heterozygous state. In absence of tamoxifen (-Tam) treatment, no recombination in the *CB1* genomic locus was observed (gel on the left). The first three lanes of the gel on the left are control reactions, representing the three possible amplification products corresponding to *wild-type*, *CB1* floxed allele, and recombined *CB1* floxed allele, respectively. **(C)** PCR for *AdipoqCreERT2* allele from tail DNA of the two mice as shown in (B), without tamoxifen (-Tam), and with tamoxifen (+Tam), indicating the presence of the transgene in both conditions, but genomic recombination occurring only in the presence of tamoxifen, as shown in (B). **(D)** Recombination in *AdipoqCreERT2* mice is restricted to adipose tissue. Cryosections from different brain regions of tamoxifen-induced *AdipoqCreERT2;ROSA26LacZ* mice were stained for β-galactosidase activity and counterstained with eosin. Brain areas shown are implicated in *CB1*-mediated regulation of food intake and energy homeostasis. Generation of mouse line, time of tamoxifen-induction and diet were as previously described (1). **(E)** Relative *CB1* mRNA levels in EF, SF, mesenteric fat (MF) and BAT at the end of the standard diet (SD) and **(F)** high-fat diet (HFD) treatment (12 weeks). *Ati-CB1-WT* (N=5-9) and *Ati-CB1-KO* (N=4-5). **(G)** Immunofluorescence detection of CB1 protein on representative paraffin-embedded sections from EF of *Ati-CB1-KO* mice before and after tamoxifen treatment (-Tam and +Tam, respectively); blue: cell nuclei; green: CB1 protein. Scale bar = 30 µm. **(H)** Relative *CB1* mRNA levels in prefrontal cortex (PFC), hypothalamus (Hypot), liver and soleus muscle (Soleus) in *Ati-CB1-WT* and *Ati-CB1-KO* mice in SD (N=3). Values are relative to *WT*. SD, standard diet; HFD, high-fat diet; Tam, tamoxifen. Data are mean ± s.e.m. Statistics: Student t-test. *, $p<0.05$; **, $p<0.01$; ***, $p<0.001$ vs. *WT*.

Supplemental Figure 2. Metabolic phenotype of *Ati-CB1-KO* mice. (A) No differences in body weight growth curves were observed between mice carrying only the *Cre recombinase* transgene, i.e., $AdipoqCreERT2^{tg/+}$ mice (N=8) and their corresponding *WT* littermates $AdipoqCreERT2^{+/+}$ (N=5) on HFD. Tamoxifen treatment was performed in the 5th week, and the switch to HFD at the beginning of the 7th week. **(B)** Blood glucose in *Ati-CB1-WT* (N=7) and *Ati-CB1-KO* (N=6-12) on standard (SD) and high-fat (HFD) diet under basal condition (after 6 hours of fasting). **(C,D)** Insulin tolerance test in *Ati-CB1-WT* (N=17-22) and *Ati-CB1-KO* mice (N=14-15) on both diet conditions. **(E)** Plasma triglycerides levels of *Ati-CB1-WT* (N=5-9) and *Ati-CB1-KO* (N=6-12) on SD and HFD. **(F)** Hepatic triglyceride content in *Ati-CB1-WT* (N=6-7) and *Ati-CB1-KO* (N=6-7) on SD and HFD. **(G)** Plasma interleukin-6 (IL6) levels of *Ati-CB1-WT* (N=5-9) and *Ati-CB1-KO* (N=6-12) on SD and HFD. Data are mean ± s.e.m. Statistics: (A,C,D) Two way ANOVA; (B,E,F) One way ANOVA; *, $p<0.05$; **, $p<0.01$; ***, $p<0.001$ vs *WT*.

Supplemental Figure 3. Adipose *CB1*-induced re-programming in different fat depots. (A) Immunofluorescence for the detection of adiponectin (adipoq) on representative paraffin-embedded sections of mesenteric fat tissue (MF) from *Ati-CB1-WT* and *Ati-CB1-KO*, both on standard (SD) and high-fat (HFD) diet. Blue: cell nuclei; red: adiponectin; scale bar: 30 µm. **(B,C)** Quantification of adipocyte cell size (arbitrary units) in epididymal (EF) and MF from *Ati-CB1-WT* (N=4) and *Ati-CB1-KO* (N=4), both on SD and HFD. **(D-G)** Gene expression analysis (relative units) in SF from *Ati-CB1-WT* and *Ati-CB1-KO* on SD (*WT*, N=4-5; *KO*, N=5-6), and HFD (*WT*, N=4-6; *KO*, N=6-10). *Cox4i2*: cytochrome c oxidase subunit IV

isoform 2; *Tfam*: mitochondrial transcription factor A; *Dio2*: iodothyronine deiodinase 2; *Elovl3*: fatty acid elongase 3. **(H)** Immunofluorescence for the detection of uncoupling protein-1 (UCP1) on representative paraffin-embedded sections of SF from *Ati-CB1-WT* and *Ati-CB1-KO*, both on SD and HFD. Blue: nuclei; green: UCP1; scale bar: 30 µm. **(I)** *Adipoq* expression (relative units) in brown adipose tissue (BAT) from *Ati-CB1-WT* and *Ati-CB1-KO* on SD (*WT,* N=7; *KO,* N=7), and HFD (*WT* N=7; *KO* N=7). Data are mean ± s.e.m. Statistics: (B-G,I) One way ANOVA; *, p<0.05; ***, p<0.001 vs *WT*.

Supplemental Figure 4. *CB1* deletion in adipocytes affects energy homeostasis. Gene expression of **(A)** pro-opiomelanocortin alpha (*Pomc*), **(B)** neuropeptide Y (*Npy*), cocaine- and amphetamine-regulated transcript (*Cartpt*), pro-melanin-concentrating hormone (*Pmch*), and (**C**) suppressor of cytokine signaling 3 (*Socs3*) in hypothalamus from *Ati-CB1-WT* (N=4-5) and *Ati-CB1-KO* (N=3-6) on SD and HFD. **(D-F)** Tissue norepinephrine levels in EF, SF and BAT from *Ati-CB1-WT* (N=6-8) *Ati-CB1-KO* (N=6-8) mice on HFD. **(G)** In vivo lipolysis induced by the β3-adrenergic receptor agonist CL316243 (0.1 mg/kg; i.p.) in *Ati-CB1-WT* (N=15) and *Ati-CB1-KO* (N=15) mice on HFD. Analysis of covariance (ANCOVA) of **(H)** energy expenditure and **(I)** resting energy expenditure (REE) during indirect calorimetry assays in *Ati-CB1-WT* (N=16) and *Ati-CB1-KO* (N=13) on HFD. Data are mean ± s.e.m. Statistics: (A-C) Two way ANOVA; (D-G) Student t-test; (H-I) ANCOVA test. *, p<0.05; **, p<0.01; ***, p<0.001 vs *WT*.

Supplemental Figure 5. Increased catecholamine synthesizing enzyme and alternatively activated macrophage expression in adipose tissue and ATMs in *Ati-CB1-KO* mice on HFD. (A) Gene expression (relative units) of catecholamine synthesizing enzymes (tyrosine hydroxylase, *Th;* dopamine beta hydroxylase, *Dbh;* dopa decarboxylase, *Ddc*) in whole EF, SF and BAT from *Ati-CB1-WT* (N=7-12) and *Ati-CB1-KO* (N=6-11) mice on HFD. **(B)** Representative flow cytometry histograms of CD206 (anti-mouse CD206-PE antibody, left panel), and CD301 (anti-mouse CD301-APC antibody, right panel) in EF from *Ati-CB1-WT* (blue), *Ati-CB1-KO* (red), and corresponding isotype control for each antibody (orange). **(C)** Representative flow cytometry experiment of CD11b+ F4/80+ adipose tissue stromal vascular cells from *Ati-CB1-WT* and *Ati-CB1-KO* mice on HFD. Numbers indicate percentage of selected cell population. **(D)** Intracellular TH protein in CD11b+ F/80+ ATMs (left panel). Representative flow cytometry histograms of TH quantification in WAT from *Ati-CB1-WT* (blue), *Ati-CB1-KO* (red), and isotype (orange). Intracellular TH protein levels in CD301+ alternatively activated M2 ATMs (right panel). Representative flow cytometry histograms of TH quantification in WAT from *Ati-CB1-WT* (blue), *Ati-CB1-KO* (red), and isotype (orange). **(E)** Immunoblot analysis of TH protein levels in spleen from *WT* and *Th-KO* mouse using the same mouse unconjugated anti-TH antibody as for flow cytometry. Number of mice per experiment is shown in brackets. Data are mean ± s.e.m. Statistics: Student t-test. *, p<0.05; **p<0.01; ***, p<0.001.

Supplemental Figure 6: Representative experiment of droplet digital PCR (ddPCR) analysis of *Th* and *Dbh* mRNA levels in CD11b$^+$ F4/80$^+$ ATMs in *Ati-CB1-WT* and *Ati-CB1-KO* mice on HFD. (A) *Th* mRNA concentration (copies/reaction) in ATMs from undiluted cDNA of *Ati-CB1-WT* and *Ati-CB1-KO* mice on HFD, adrenal gland as positive control (dilution 1:1000 of cDNA), and negative control (NTC: H_2O). **(B)** *Dbh* mRNA concentration (copies/reaction) in ATMs from *Ati-CB1-WT* and *Ati-CB1-KO* mice on HFD, adrenal gland as positive control (dilution 1:1000 of cDNA), and negative control (NTC: H_2O). **(C)** *Dbh* and *Th* mRNA concentration (copies/reaction) in two positive samples: adrenal gland (dilution 1:1000 of cDNA) and brainstem (dilution 1:100 of cDNA), and two negative control samples: no-RT adrenal glands (dilution 1:1000 of no-RT RNA), and negative control (NTC: H_2O).

Supplemental Figure 7: Immunoperoxidase staining of TH-positive noradrenergic nerve fibers in adipose tissue from HFD-fed *Ati-CB1-WT* and *Ati-CB1-KO* mice on HFD. (A) In the interscapular BAT of *Ati-CB1-WT* mice, brown adipocytes are enlarged and contain

large and coalescing lipid droplets; parenchymal noradrenergic nerve fibers (arrowheads) are rarely detectable. **(B)** In contrast, interscapular brown adipocytes from *Ati-CB1-KO* mice are smaller and filled with small and numerous lipid droplets; parenchymal noradrenergic nerve fibers (arrowheads) are frequently detectable among them; in the lower right corner of B, note also the presence of an artery (A) richly decorated with noradrenergic innervation. **(C)** In SF from control mice, a noradrenergic nerve fiber (arrow) is associated with a capillary (cap), and another noradrenergic nerve fiber (arrowhead) is in close apposition to a white adipocyte. **(D)** In SF of *Ati-CB1-KO*, a higher number of parenchymal noradrenergic nerve fibers (arrowheads) are visible in close apposition to adipocytes. Note also the reduced size of adipocytes in *Ati-CB1-KO*, which also show some signs of rearrangement of their lipid content and multilocularity. In bar graphs, quantification of TH+ fibers per 200 adipocytes in BAT and SF from *Ati-CB1-KO* mice. Number of mice per experiment is shown in brackets. Scale bar: for A and B 50 µm; for C and D 30 µm.

Supplemental Figure 8: Double staining and confocal microscopy analysis of interscapular BAT and subcutaneous WAT (SF) from HF-fed *Ati-CB1-KO* mice. (A) CD206+ macrophage body (M) and macrophage elongated projections (Mp) are visible as red structures. **(B)** In the same confocal section, tyrosine hydroxylase (TH)+ parenchymal noradrenergic nerve fibers are detectable (arrowheads, green structures). **(C)** Nuclei were stained with TO-PRO3. **(D)** As evident in the merged image, a tight anatomical proximity (arrows) between CD206+ macrophage bodies or projections and noradrenergic nerve fibers is frequently detectable. For BAT, two areas of this confocal section were enlarged in the insets to better appreciate the close spatial relationship, but not colocalization, between the neuronal and macrophage structures. Scale bar: 25 µm; insets 8 µm.

Supplemental Figure 9. Phenotypic analysis under thermoneutrality (30°C) conditions. (A) Body weight growth curves and **(B)** food consumption of *Ati-CB1-WT* (N=7-8) and *Ati-CB1-KO* (N=8-14) on HFD at regular animal housing temperature (22°C) and at thermoneutrality (30°C). **(C)** Gene expression (relative units) of thermogenesis markers (uncoupling protein 1, *Ucp1;* fatty acid elongase 3*, Elovl3*) in BAT from 22°C/*Ati-CB1-WT* (N=8), 30°C/*Ati-CB1-WT* (N=6), and 30°C/*Ati-CB1-KO* (N=10). **(D)** Gene expression (relative units) for *Ucp1*, peroxisome proliferator-activated receptor gamma coactivator 1 alpha (*Ppargc1a*), cytochrome c oxidase VIIIb (*Cox8b*) and mitochondrial transcription factor A (*Tfam*), and for markers for alternatively activated macrophages (*Clec10a, Mrc1*) and catecholamine synthesizing enzyme (dopa decarboxylase, *Ddc*) in SF from 22°C/*Ati-CB1-WT* (N=8), 30°C/*Ati-CB1-WT* (N=6), and 30°C/*Ati-CB1-KO* (N=10). **(E)** Gene expression (relative units) of markers for alternatively activated macrophages (*Clec10a, Mrc1*) and the catecholamine synthesizing enzyme *Ddc* in BAT of *Ati-CB1-WT* (N=7-8) and *Ati-CB1-KO* (N=10) on HFD at animal housing temperature (22°C) and at thermoneutrality (30°C). Data are mean ± s.e.m. Statistics: (A) Two way ANOVA; (B-E) One way ANOVA; (A,B). *, $p<0.05$ vs 30°C/*WT*; # $p<0.05$ vs 22°C/*WT*, **$p<0.01$ 22°C vs 30°C; (B-E) *, $p<0.05$, **$p<0.01$, ***, $p<0.001$.

Supplemental Figure 10. Adipose *CB1 receptor* deletion induced alternatively macrophage activation, preceding the emergence of body weight differences. Representative flow cytometry histograms of (**A**) CD206 (anti-mouse CD206-PE antibody) and (**B**) CD301 (anti-mouse CD301-ACP antibody) in EF from 7 week-old *Ati-CB1-WT* (in blue), *Ati-CB1-KO* (in red), and corresponding isotype control for each antibody (orange) i.e., 2 weeks after tamoxifen-induced *CB1 receptor* deletion in adipocytes.

Supplemental Figure 11. Inducible *CB1* deletion in the adult mice under SD and super-HFD (SHFD). (A,B) After tamoxifen treatment in week 16 of age, *Ati-CB1-KO-TAO* showed a significant reduction of *CB1* mRNA levels in epididymal (EF), subcutaneous (SF), mesenteric (MF) and brown (BAT) adipose tissue, on both SD and HFD at week 22 of age. **(C)** *Ati-CB1-KO-TAO* on SD did not show any significant reduction in the total amount of EF and SF, while **(D)** analysis of adipose tissue weight revealed that differences in body weight between

Ati-CB1-WT-TAO and *Ati-CB1-KO-TAO* on SHFD and their *WT* were caused by strong reduction in the total amount of both EF and SF. **(E)** Histology of SF, EF and BAT from *Ati-CB1-KO-TAO* and *Ati-CB1-WT-TAO* mice on SHFD. Scale bar = 30 µm. **(F)** Chronic treatment with the peripheral CB1 antagonist AM6545 (10 mg/kg, i.p.) or its vehicle, and analysis of weekly food intake in *Ati-CB1-KO-TAO* (N=6) and *Ati-CB1-WT-TAO* (N=8-7) on SHFD. Data are mean ± s.e.m. Statistics: (A-D) Student t-test. *Ati-CB1-WT-TAO* (N=8-10) and *Ati-CB1-KO-TAO* (N=6-7), (F) Two way ANOVA, Bonferroni post-hoc test. (F-H): Two way ANOVA *, p<0.05; **, p<0.01; ***, p<0.001.

Supplemental Figure 12. *CB1* inactivation in adipocytes prevents obesity-related anxiety-like behaviors. (A) Total locomotion tested in the open field test is not affected in none of the experimental groups. **(B)** In the elevated plus maze, percentage of entries into the open arms (OA; a parameter inversely correlated with the level of anxiety of the subject) and **(C)** percentage of time in the OA, both parameter were significantly lower in obese *Ati-CB1-WT-TAO* fed with SHFD than in *Ati-CB1-WT-TAO* in SD. This diet-induced effect is absent in *Ati-CB1-KO-TAO* fed with SHFD. **(D)** In the holeboard test, the level of exploration was decreased in the *Ati-CB1-WT-TAO* under SHFD and unchanged in *Ati-CB1-KO-TAO* as compared to mice in SD. Data are mean ± s.e.m. Statistics: Two way ANOVA. *, p<0.05; **, p<0.01; ***, p<0.001.

Reference

1. Sassmann,A., Offermanns,S., and Wettschureck,N. 2010. Tamoxifen-inducible Cre-mediated recombination in adipocytes. *Genesis.* **48**:618-625.

Supplemental Figure 1

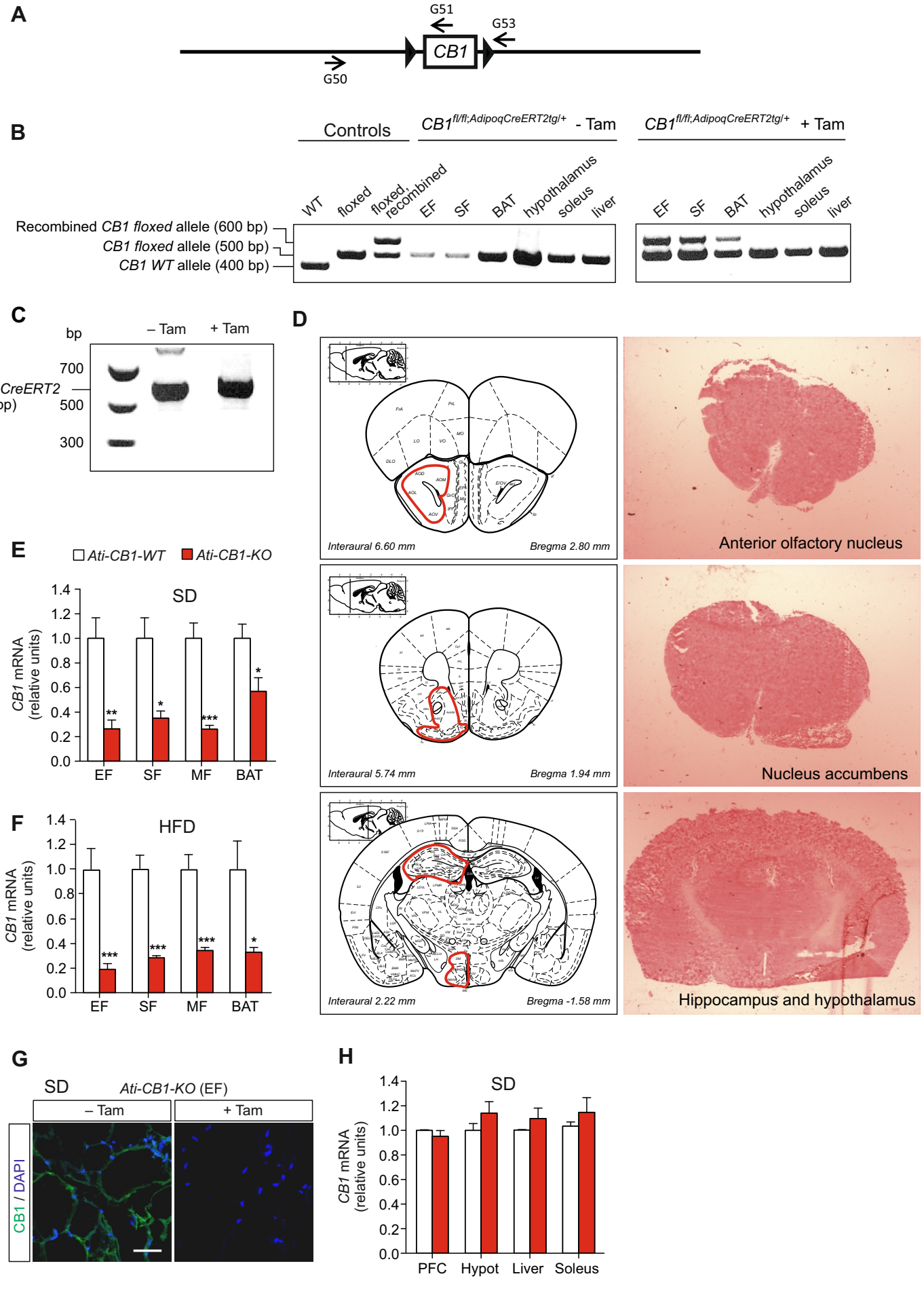

Supplemental Figure 2

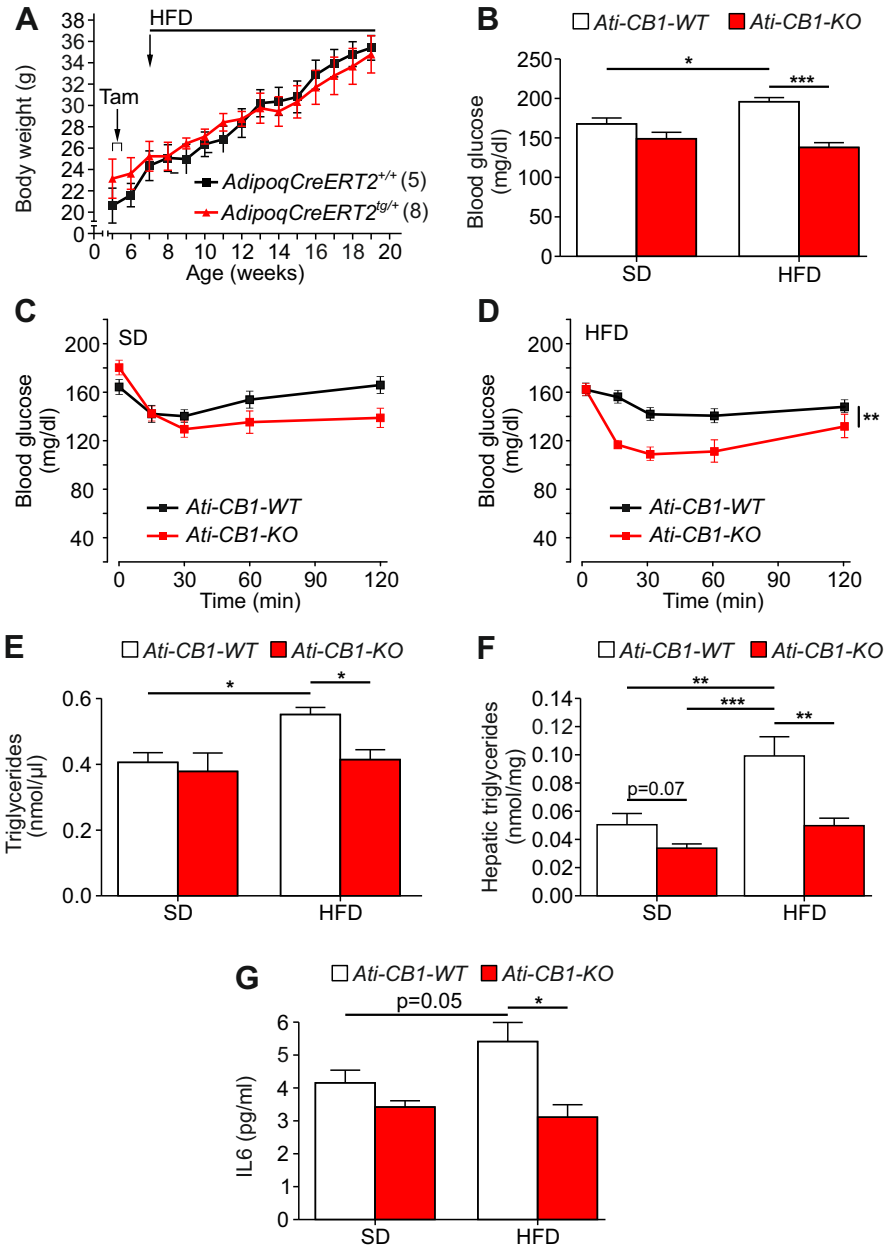

Supplemental Figure 3

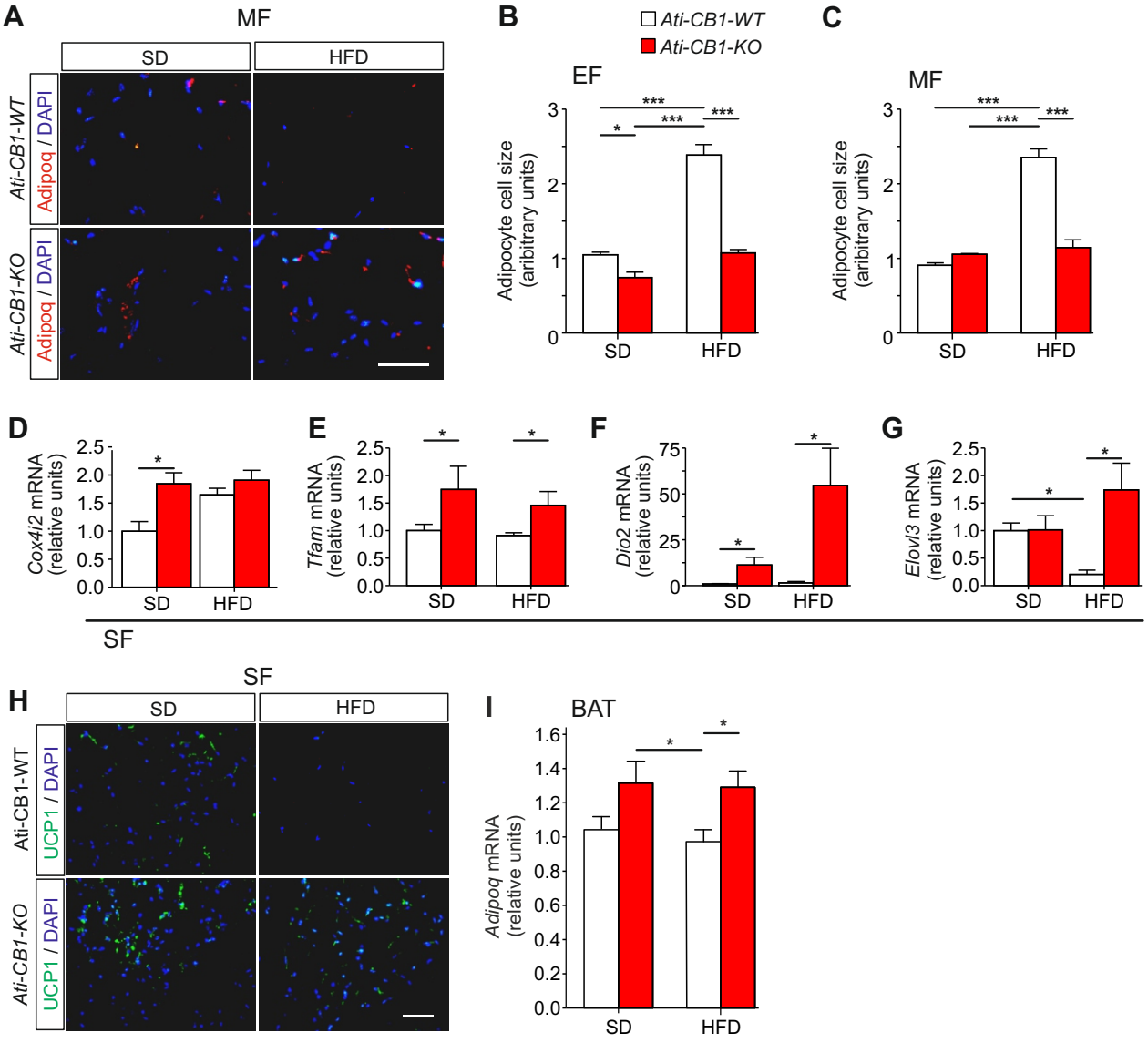

Supplemental Figure 4

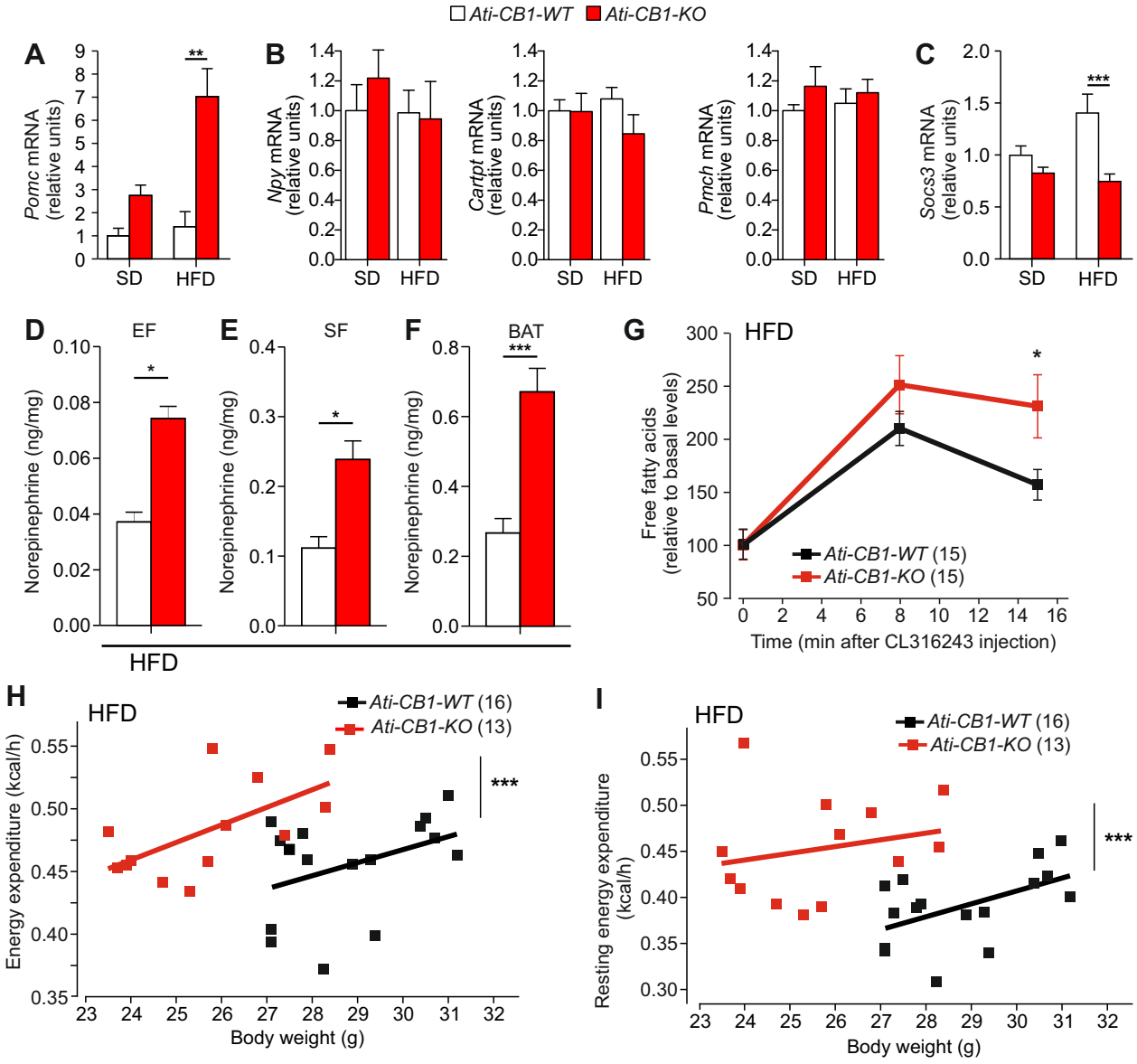

Supplemental Figure 5

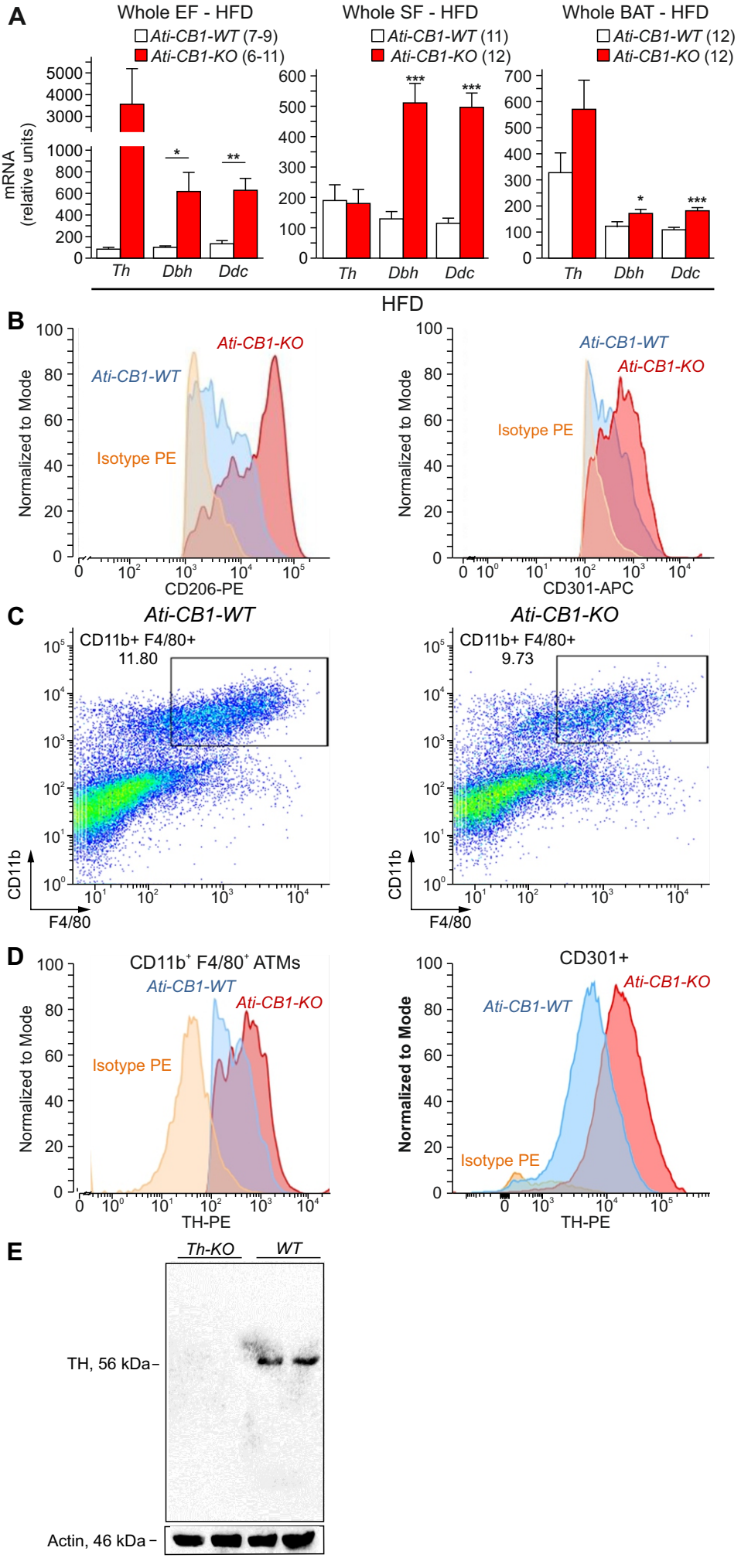

Supplemental Figure 6

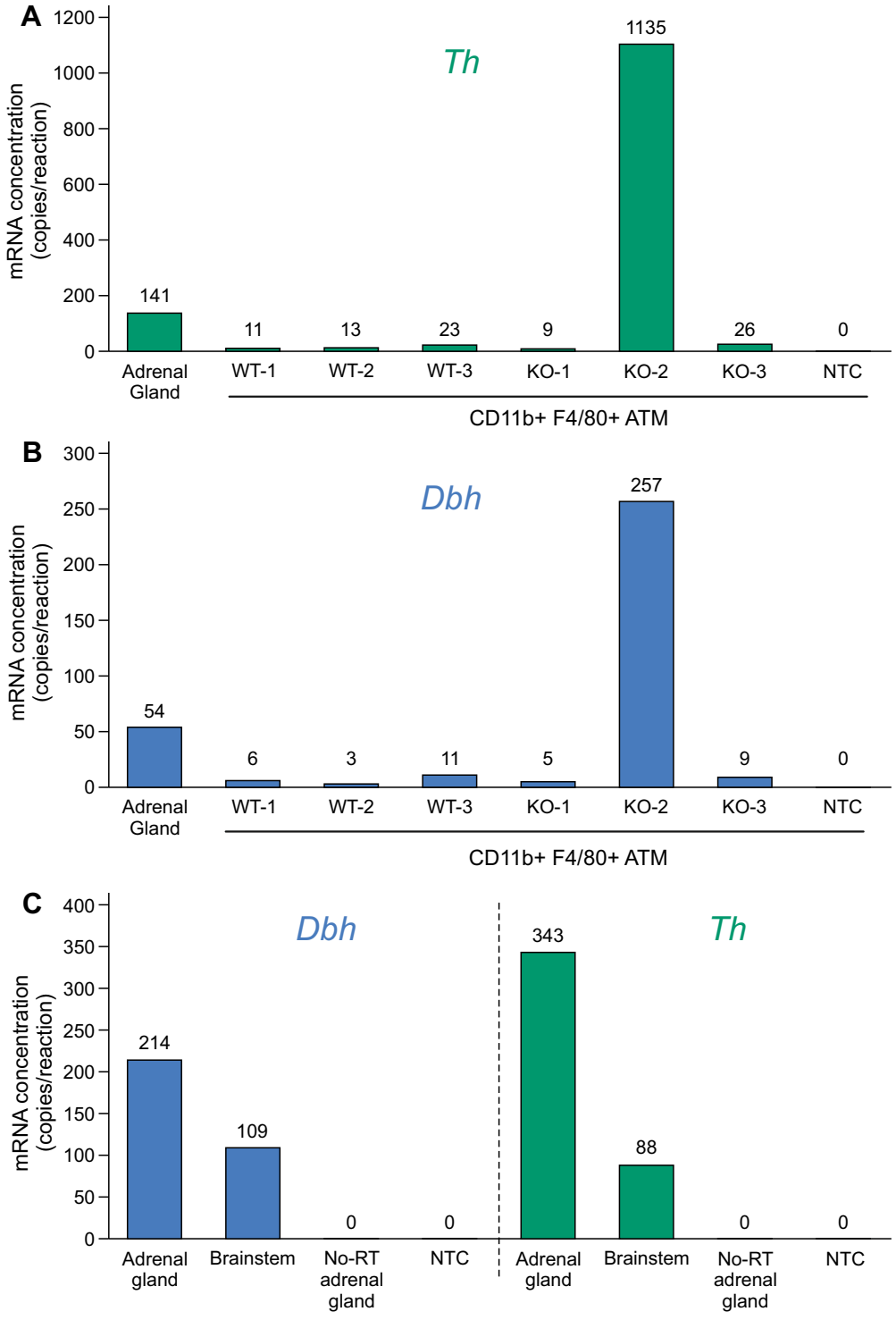

Supplemental Figure 7

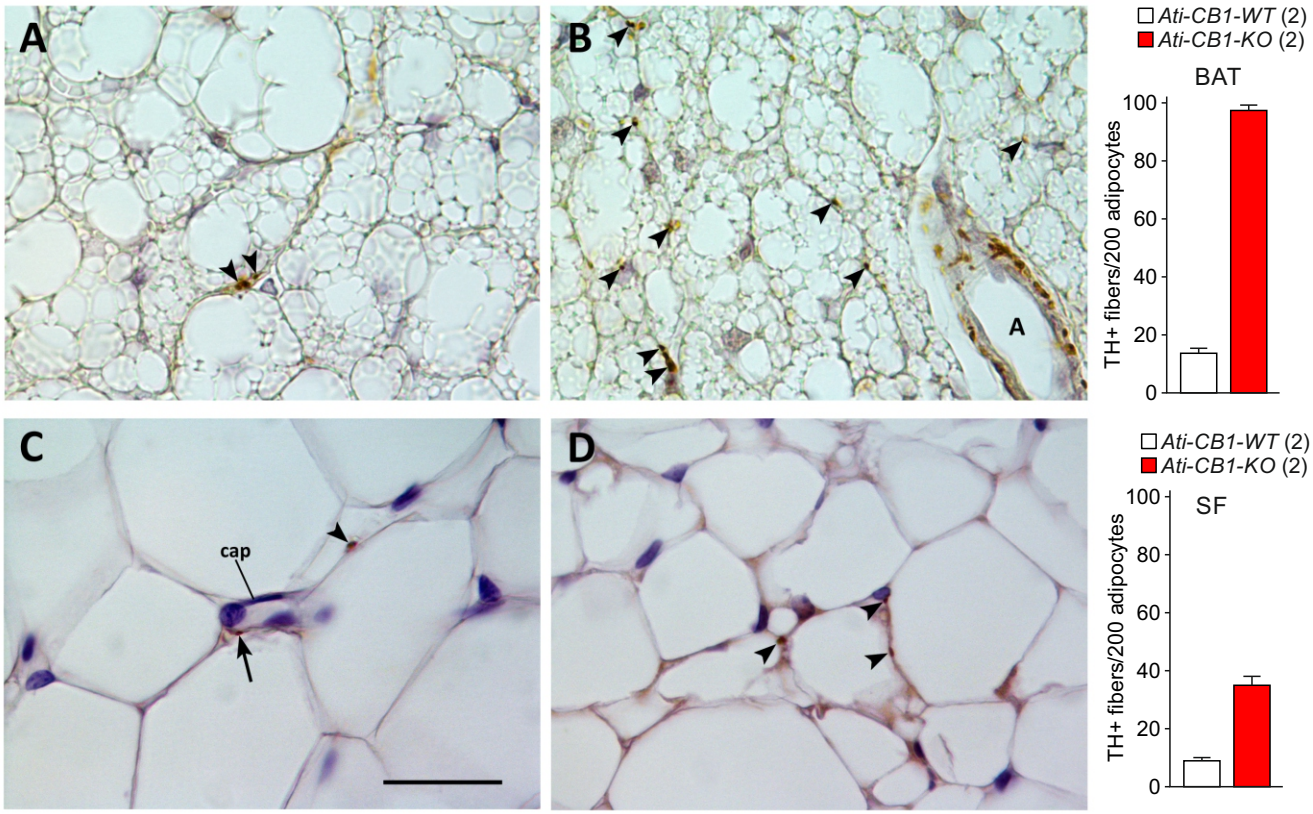

Supplemental Figure 8

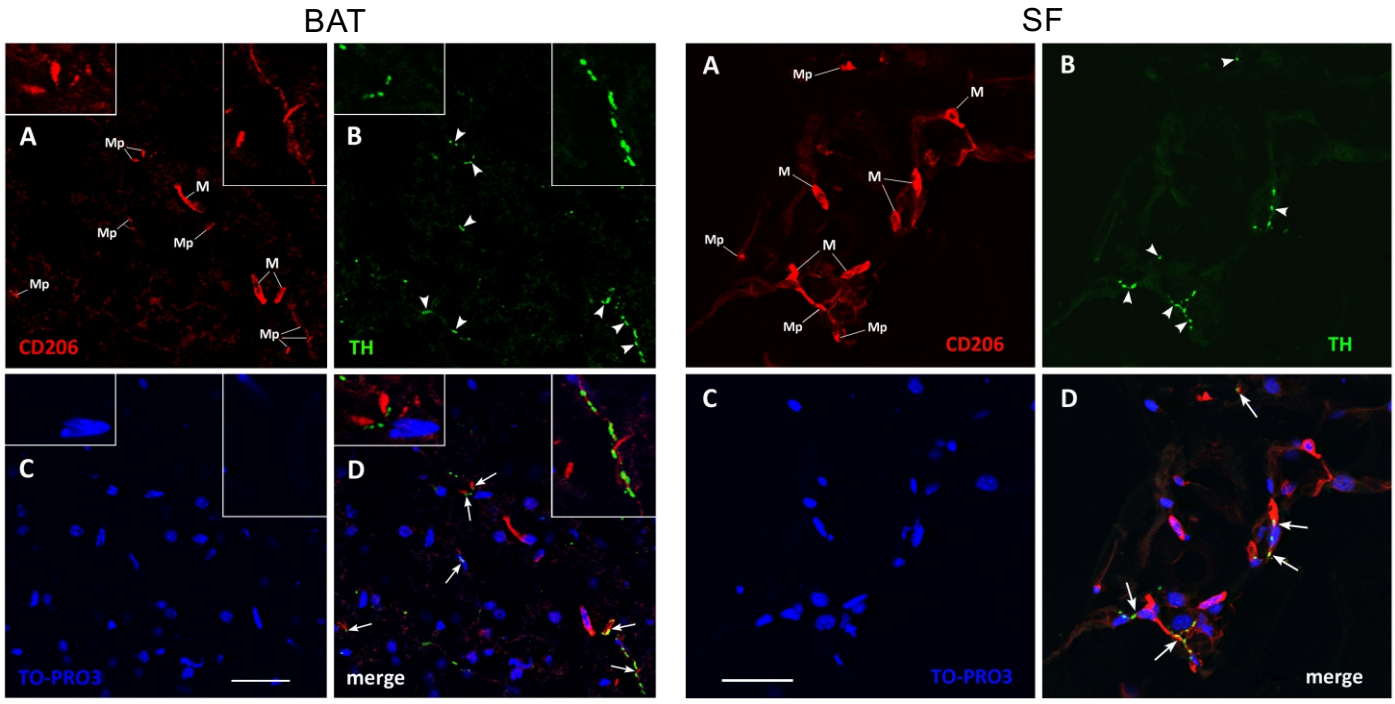

Supplemental Figure 9

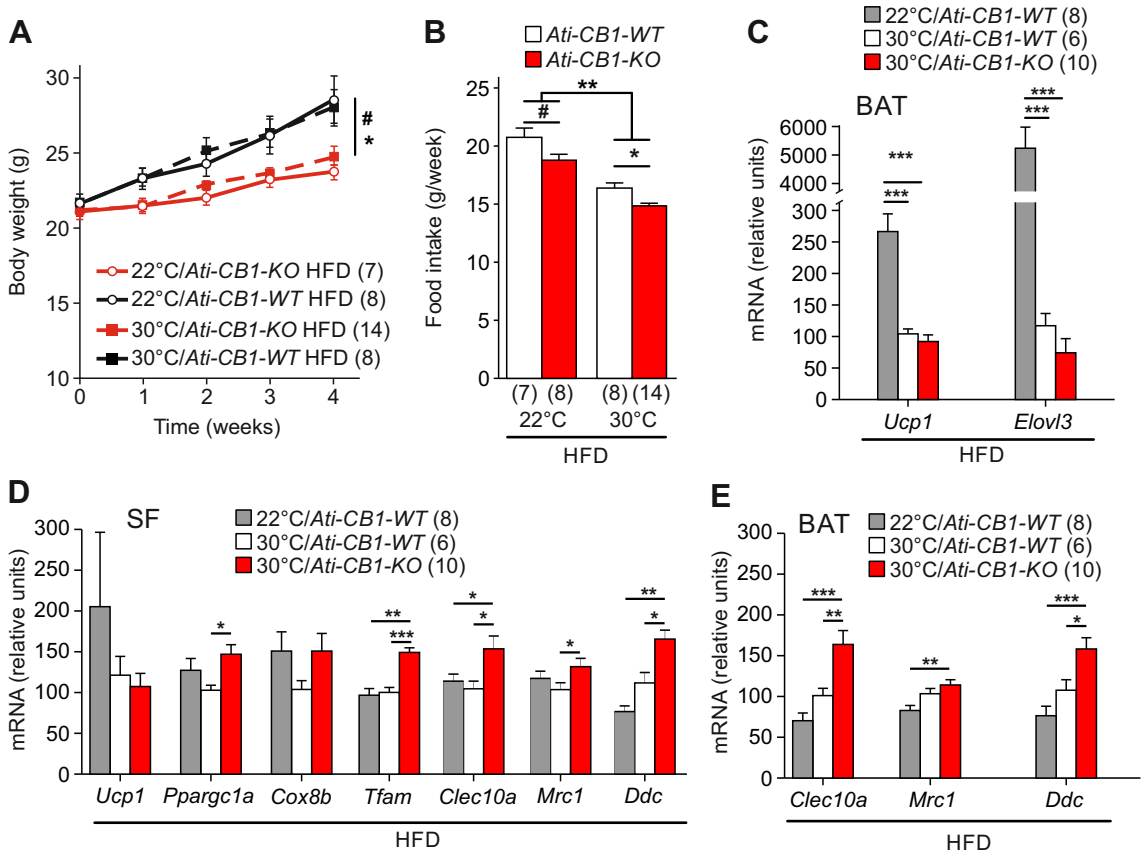

Supplemental Figure 10

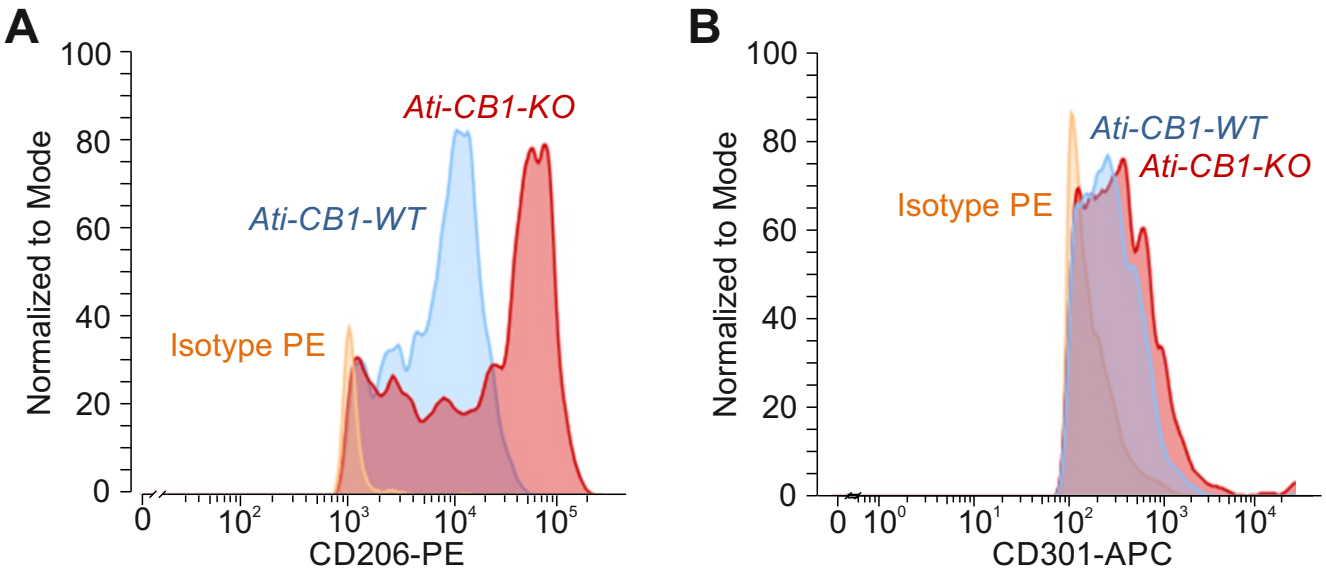

Supplemental Figure 11

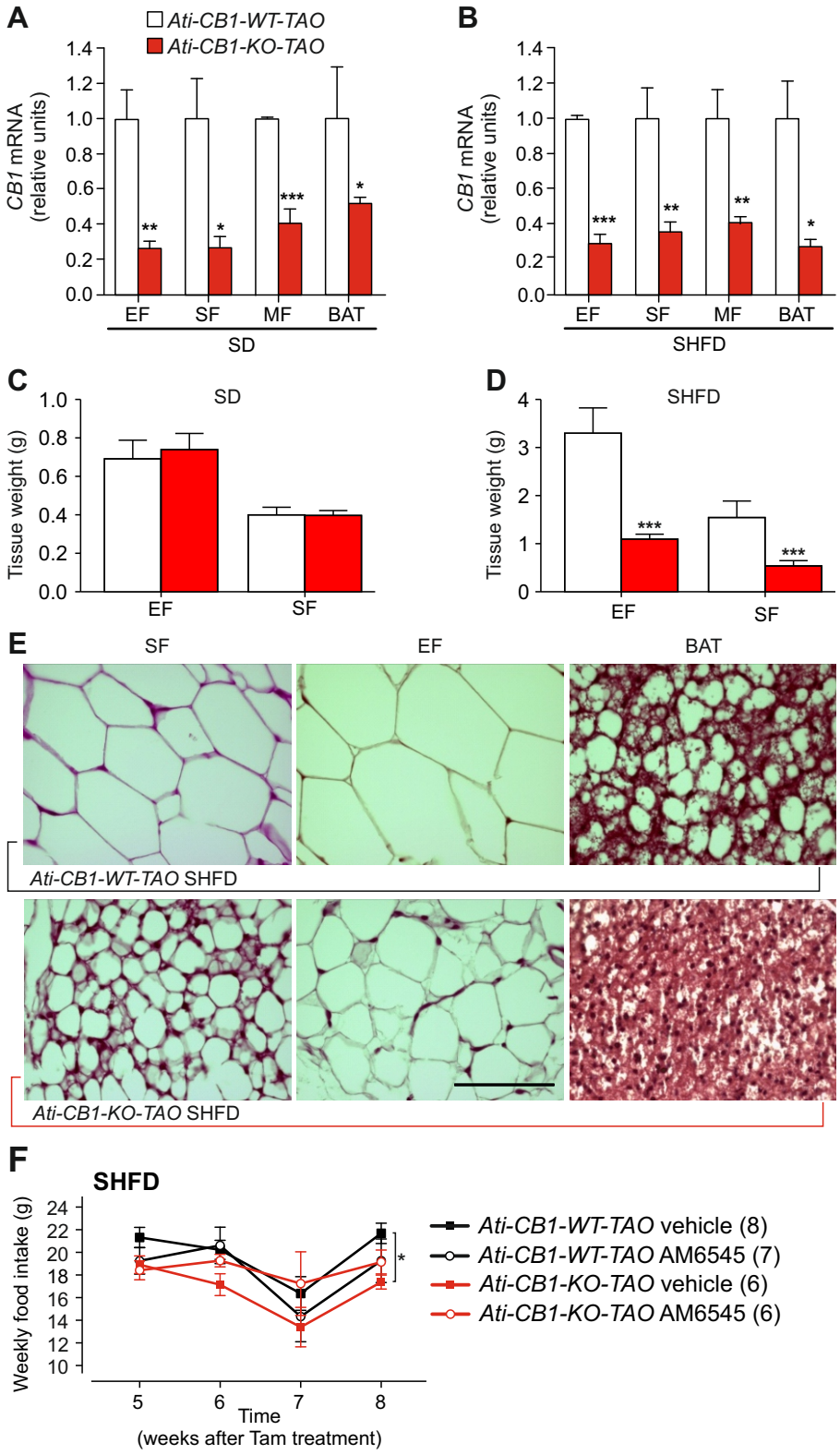

Supplemental Figure 12